

SIMCor

In-Silico testing and validation of Cardiovascular IMplantable devices

Call: H2020-SC1-DTH-2018-2020 (*Digital transformation in Health and Care*)

Topic: SC1-DTH-06-2020 (*Accelerating the uptake of computer simulations for testing medicines and medical devices*)

Grant agreement No: 101017578

Deliverable 7.5

Uncertainty quantification and re-definition of input space

Due date of delivery: 30 June 2022

Actual submission date: 30 June 2022

Start of the project: 1 January 2021

End date: 31 December 2023



Reference

Name	SIMCor_D7.3_Definition of input space_TUE_28-09-2021
Lead beneficiary	Technische Universiteit Eindhoven (TUE)
Author(s)	Wouter Huberts (TUE)
Dissemination level	Public
Type	Report
Official delivery date	30 June 2022
Date of validation by the WP Leader	30 June 2022
Date of validation by the Coordinator	30 June 2022
Signature of the Coordinator	

Version log

Issue date	Version	Involved	Comments
23/06/2022	1.0	Wouter Huberts (TUE)	First draft by TUE
27/06/2022	2.0	Jan Brüning (CHA); Michael Stiehm (IIB), Finja Borowski (IIB), Jan Oldenburg (IIB)	Internal review by CHA and IIB
30/06/2022	3.0	Wouter Huberts (TUE)	New version, taking into accounts comments and suggestions
30/06/2022	4.0	Anna Rizzo (LYN)	Final review and formal checking by LYN
30/06/2022	Final	Jan Brüning (CHA)	Submission by PC

Executive summary

This deliverable demonstrates how the sensitivity analyses described in *D7.4 - Sensitivity and uncertainty quantification toolbox (TUE, M15)* can be used to re-define the input space. Three possible objectives regarding input space re-definition are considered: 1) reducing the number of parameters that span the input space (i.e., dimensionality reduction by parameter fixing) to facilitate amongst other physiological model development and future model output uncertainty quantification; 2) reducing the input uncertainty domains of the model parameters, boundary conditions and/or model assumptions that will lead to the most significant reduction in model output uncertainty (parameter prioritisation); 3) defining the regions of the input space that result in parameter sets that lead to physiologically realistic realisations of the virtual cohort generator.

This deliverable starts with a summary of the most important definitions and background of the uncertainty and sensitivity analyses discussed in D7.4. Thereafter, we will show how these sensitivity analysis techniques are applied to address the three different objectives above. In this deliverable three models, possible candidates for virtual cohort generation of the SIMCor use cases (i.e., aortic valve stenosis and heart failure patients), are selected as typical examples. Finally, the future steps towards virtual cohort generation and validation are discussed.

Table of contents

DEFINITIONS	4
UNCERTAINTY QUANTIFICATION AND INPUT SPACE RE-DEFINITION	6
DIMENSIONALITY REDUCTION OF THE INPUT SPACE	6
<i>Study setup</i>	7
<i>Results and discussion</i>	8
RE-DEFINITION OF INPUT UNCERTAINTY DOMAINS	9
<i>Study setup</i>	9
<i>Results and discussion</i>	10
RE-DEFINITION OF INPUT SPACE FOR VIRTUAL COHORT GENERATION	13
<i>Study setup</i>	13
<i>Results and discussion</i>	14
NEXT STEPS TOWARDS VIRTUAL COHORT GENERATION	16

List of figures

FIGURE 1: DEFINITION OF UNCERTAINTY AND SENSITIVITY ANALYSIS. BASED ON SALTELLI ET AL. ^{1,2}	5
FIGURE 2: SCHEMATIC REPRESENTATION OF THE REGIONALIZED SENSITIVITY ANALYSIS THAT IS USED TO IDENTIFY SELECTION CRITERIA OF THE FILTER. THE FILTERED SAMPLES ULTIMATELY RESULT IN A RE-DEFINITION OF THE VIRTUAL COHORT INPUT SPACE.	6
FIGURE 3: THE DIFFERENCES BETWEEN THE MAIN AND TOTAL SENSITIVITY INDICES, WHICH ARE REPRESENTATIVE FOR THE CONTRIBUTION OF INPUTS ON THE OUTPUT VARIANCE VIA INTERACTIONS WITH OTHER INPUTS.	7
FIGURE 4: THE SENSITIVITY INDICES, THE EXPECTED VALUE, AND THE OUTPUT VARIANCE FOR THE FIRST SENSITIVITY ANALYSIS WITH THE MEAN TIME AVERAGED WSS AS OUTPUT OF INTEREST.	8
FIGURE 5: THE SENSITIVITY INDICES, THE EXPECTED VALUE, AND THE OUTPUT VARIANCE FOR THE SECOND SENSITIVITY ANALYSIS (AND THUS A RE-DEFINED INPUT SPACE) WITH THE MEAN TIME AVERAGED WSS AS OUTPUT OF INTEREST.	8
FIGURE 6: THE SENSITIVITY INDICES, THE EXPECTED VALUE, AND THE OUTPUT VARIANCE FOR THE FIRST SENSITIVITY ANALYSIS WITH THE MAXIMUM PRESSURE AS OUTPUT OF INTEREST.	9
FIGURE 7: THE SENSITIVITY INDICES, THE EXPECTED VALUE, AND THE OUTPUT VARIANCE FOR THE SECOND SENSITIVITY ANALYSIS (AND THUS THE RE-DEFINED INPUT SPACE) WITH THE MAXIMUM PRESSURE AS OUTPUT OF INTEREST.	9
FIGURE 8: THE SETUP OF THE MODEL USED FOR THE UNCERTAINTY AND SENSITIVITY ANALYSIS. TOP: THE GEOMETRY AND THE PRESSURE SENSOR INSERTED, BOTTOM: EXEMPLARY RESULTS OF WALL SHEAR STRESSES PRESENT.	10
FIGURE 9: THE SENSITIVITY INDICES, THE EXPECTED VALUE, AND THE OUTPUT VARIANCE FOR THE FIRST SENSITIVITY ANALYSIS WITH THE AREA OF LOW WSS AS OUTPUT OF INTEREST.	11
FIGURE 10: THE SENSITIVITY INDICES, THE EXPECTED VALUE, AND THE OUTPUT VARIANCE FOR THE SECOND SENSITIVITY ANALYSIS (AND THUS THE RE-DEFINED INPUT SPACE) WITH THE AREA OF LOW WSS AS OUTPUT OF INTEREST.	11
FIGURE 11: BOXPLOTS SHOWING THE SIMULATION DATA THAT WAS INPUT FOR THE AGPCE. NOTE THE OUTLIERS IN ESPECIALLY THE DATA SET OF THE FIRST UNCERTAINTY AND SENSITIVITY ANALYSIS (LEFT).	12
FIGURE 12: THE SENSITIVITY INDICES, THE EXPECTED VALUE AND THE OUTPUT VARIANCE FOR THE FIRST SENSITIVITY WITH THE FORCE APPLIED TO THE SENSOR AS OUTPUT OF INTEREST.	12
FIGURE 13: THE SENSITIVITY INDICES, THE EXPECTED VALUE, AND THE OUTPUT VARIANCE FOR THE SECOND SENSITIVITY (AND THUS THE RE-DEFINED INPUT SPACE) WITH THE FORCE APPLIED TO THE SENSOR AS OUTPUT OF INTEREST.	13
FIGURE 14: A SCHEMATIC PICTURE OF THE VIRTUAL COHORT GENERATOR (LEFT) AND A TYPICAL EXAMPLE OF A VIRTUAL PATIENT, I.E., A GEOMETRY, A PHYSIOLOGICAL MODEL AND PROPER PARAMETERS/BOUNDARY CONDITIONS (RIGHT).	14
FIGURE 15: A PARALLEL ORTHOGONAL PLOT SHOWING THE 10 TH TO 90 TH PERCENTILE INTERVALS FOR ALL COMPONENTS OF THE INPUT SAMPLES AND THE CORRESPONDING MODEL OUTPUT REALISATIONS. THESE INTERVALS ARE GIVEN FOR BOTH REALISTIC AND UNREALISTIC MODEL OUTPUTS.	15
FIGURE 16: A PARALLEL ORTHOGONAL PLOT SHOWING THE 25 TH TO 75 TH PERCENTILE INTERVALS FOR ALL COMPONENTS OF THE INPUT SAMPLES AND THE CORRESPONDING MODEL OUTPUT REALISATIONS. THESE INTERVALS ARE GIVEN FOR BOTH REALISTIC AND UNREALISTIC MODEL OUTPUTS.	15
FIGURE 17: THE NUMBER OF UNREALISTIC MODEL REALISATIONS. ON THE LEFT THE SITUATION WITHOUT RE-DEFINITION OF THE INPUT SPACE, WHEREAS THE MIDDLE AND RIGHT ILLUSTRATE THE FRACTION OF UNREALISTIC SIMULATIONS AFTER RE-DEFINING THE INPUT SPACE BASED ON THE 10 TH -90 TH PERCENTILE AND 25 TH -75 TH PERCENTILE INTERVAL OF PARAMETER A ₁ .	16

List of tables

TABLE 1: INPUT RANGES FOR THE UNCERTAINTY AND SENSITIVITY ANALYSIS (PARAMETER FIXING). 8

TABLE 2: INPUT RANGES FOR THE UNCERTAINTY AND SENSITIVITY ANALYSIS (PARAMETER PRIORITISATION). 10

Acronyms

Acronym	Full name
RSA	Regionalized Sensitivity Analysis
RPA	Right Pulmonary Artery
LPA	Left Pulmonary Artery
MPA	Main Pulmonary Artery

Definitions

In this section we briefly repeat the uncertainty and sensitivity analysis techniques that will be used in this deliverable for re-definition of the input space. The methods were extensively described in D7.4. **Variance-based sensitivity analysis**^{1,2}: in this method the model output uncertainty due to uncertainties in model inputs is quantified by the output variance. Subsequently, each fraction of the total uncertainty in model outputs is attributed to uncertainties of the inputs and/or the interactions between uncertain inputs (see *Figure 1*).

The main Sobol sensitivity index represents the contribution of an input on its own to the total output variance, whereas the total Sobol sensitivity index also considers the interactions in which an input is involved.

Since the main sensitivity index of a single input can be interpreted as the expected reduction in output variance when the exact value of the input would have been known, this index can be used to select the inputs that are most rewarding to assess more accurately (input factor prioritisation). In this way, these indices can guide the measurement protocol for model personalisation during the phases of model development and patient-level validation.

The total index of a single input factor can be interpreted as the expected variance that is left if all other inputs were set to their real (exact) values. In this way, the total index can help in identifying those inputs that can be fixed within their uncertainty domain (factor fixing).

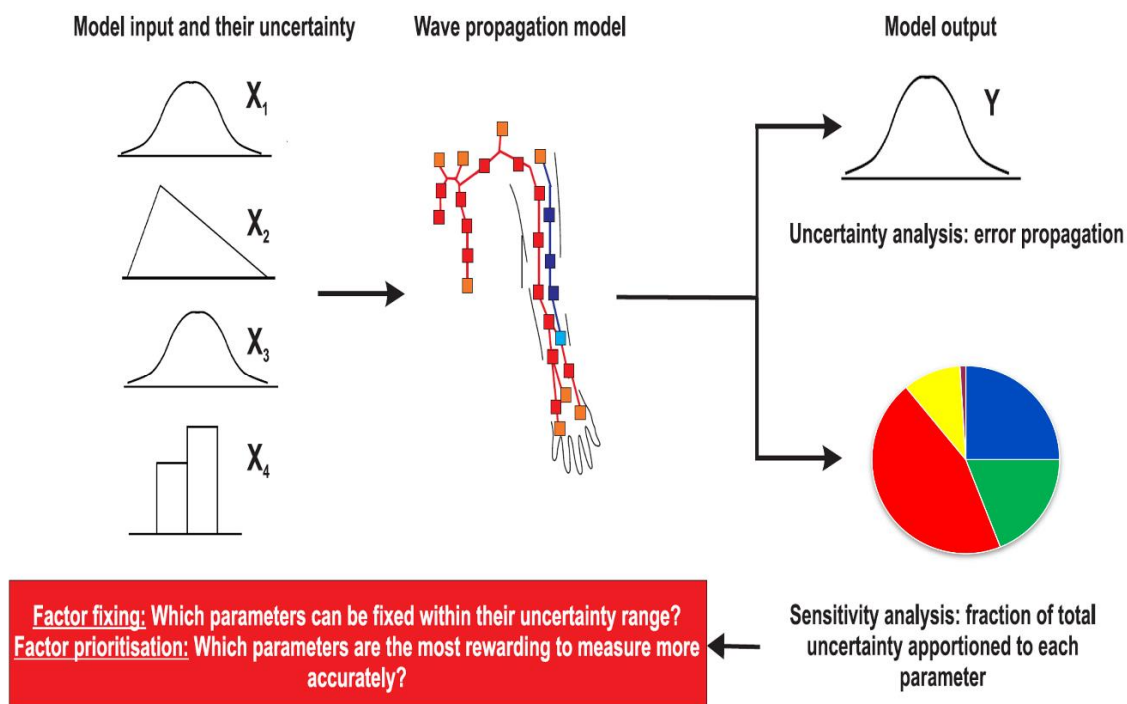


Figure 1: Definition of uncertainty and sensitivity analysis. Based on Saltelli et al.^{1,2}.

Here we applied the adaptive, generalized polynomial chaos expansion method that was firstly introduced by Blatman et al.³ and later applied to cardiovascular problems by Quicken et al.⁴ To efficiently calculate these indices we have used the implementation of QuGate (<https://qugate.nl/>).

¹ Saltelli et al., 2019, <https://doi.org/10.1016/j.envsoft.2019.01.012>

² Saltelli et al., 2004, Sensitivity analysis in practice: a guide to assessing scientific models, ISBN 0-470-87093-1

³ Blatman et al., 2010, <https://doi.org/10.1016/j.j.ress.2010.06.015>

⁴ Quicken et al., 2016, <https://doi.org/10.1115/1.4034709>

Regionalized sensitivity analysis: this method, also called Monte Carlo filtering, is used to determine which model assumptions, structures or combination of model inputs are responsible for model output realisations in specific areas of the output space (i.e., the realisations that are within a region classified as acceptable according to predefined acceptance criteria)^{5,6}. The schematic in *Figure 2* depicts the basic idea of this type of sensitivity analysis.

In the context of SIMCor, this approach will primarily be used during virtual cohort generation for defining the filter setting, i.e., the criteria to determine whether a virtually created patient is realistic or not.

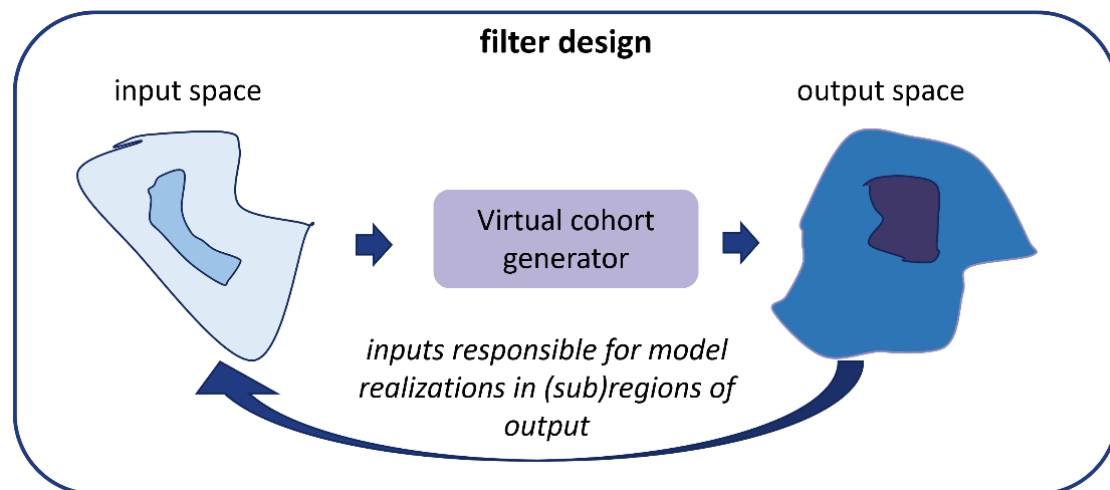


Figure 2: Schematic representation of the regionalized sensitivity analysis that is used to identify selection criteria of the filter. The filtered samples ultimately result in a re-definition of the virtual cohort input space.

In this deliverable we will analyse the region of the input space that gives output realisations in the output space of interest, i.e., the distribution of the input samples that are filtered out and considered realistic.

⁵ Pianosi et al., 2016, DOI: 10.1016/j.envsoft.2016.02.008

⁶ Saltelli et al., 2004, Sensitivity analysis in practice: a guide to assessing scientific models, ISBN 0-470-87093-1

Uncertainty quantification and input space re-definition

Dimensionality reduction of the input space

In this section we will show that the dimensionality of the input space for a patient-specific model can be reduced by using the variance-based sensitivity analysis, without significantly affecting the estimations of the expected value of the model output and its uncertainty (variance). The total indices can be used to identify the set of parameters (inputs) that can be set to a constant value within their uncertainty domain, thereby reducing the number of parameters that have an input variation and thus the dimensionality of the input space. In addition, we will show that fixing the wrong parameter to a value within the population uncertainty domain, would affect the estimates of the expected value and the variance.

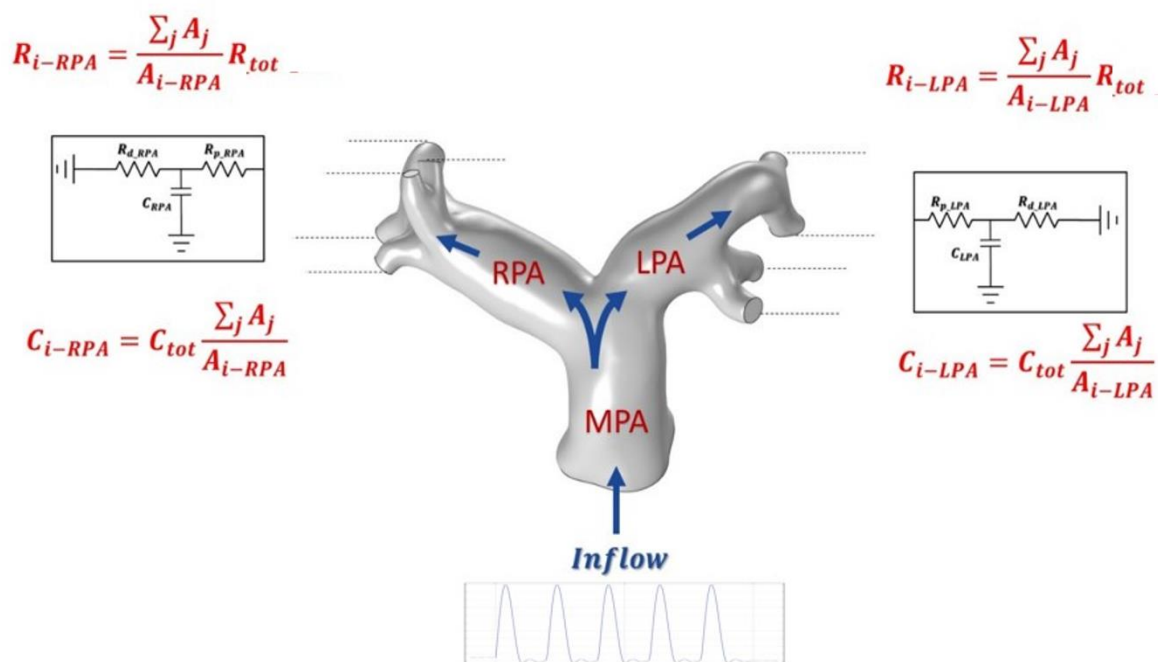


Figure 3: The setup of the model used for the uncertainty and sensitivity analysis. The main, left and right pulmonary arteries are presented in 3D, whereas distal vasculatures are mimicked by Windkessel models.

Study setup

A variance-based sensitivity analysis (and uncertainty analysis) using the agPCE method (see D7.4) is applied to a 3D CFD model of the main, left and right pulmonary arteries (see Figure 3). The input impedance of the distal vasculatures at the outlets of the *left pulmonary artery* (LPA) and the *right pulmonary artery* (RPA) were mimicked by three-element Windkessel models. At the inlet of the *main pulmonary artery* (MPA) a typical inlet flow waveform was applied by means of a transient plug velocity profile. The 3D computational domain consisted, after mesh independency analysis, of 1.3 million tetrahedral volumetric mesh elements with an average quality of 0.68. Blood flow was considered as a laminar, incompressible, and blood was modelled as Newtonian fluid. Dynamic blood viscosity and blood density were set to $3.5 \cdot 10^{-3}$ [Pa · s] and 1065 [kg/m³], respectively. The 3D transient pressure and velocity fields within the computational domain were calculated by using COMSOL Multiphysics. These output data are subsequently processed and converted to two scalar outputs that are examined during the uncertainty and sensitivity analysis in this study, i.e., the mean time-averages wall shear stress (MTAWSS) and the maximum arterial pressure (p_{max}).

To quantify the value of the outputs and their corresponding uncertainties, the expected values and the output variances are estimated. In addition, the main and total sensitivity indices are calculated. Two different analyses are executed: 1) an initial uncertainty and sensitivity analysis (SA1) and 2) a second one (SA2) but now with a re-defined input space based on the total sensitivity indices (very low values indicate that we can fix the respective parameters within their uncertainty domain).

The input space for the uncertainty and sensitivity analysis was spanned by four uncertain inputs: stroke volume, heart rate, total peripheral resistance, and the total distal arterial compliance. The input ranges were defined as presented in *Table 1*.

Input parameter	Ranges SA1	Ranges SA2
#1: Heart Rate [bpm]	50 -120 ⁷	50-120
#2: Stroke Volume [ml]	50 – 100 ⁸	50-100
#3: Total Resistance [dynes/s/cm ⁵]	50 – 250 ⁹	constant value = 150
#4: Total Compliance [ml/mmHg]	0.75 – 3 ¹⁰	constant value = 1.875

Table 1: Input ranges for the uncertainty and sensitivity analysis (parameter fixing).

Results and discussion

In *Figure 4* the results of the uncertainty and sensitivity analysis for MTAWSS are presented. Here it can be observed that the expected value for the MTAWSS is estimated to be 2.3 Pa, whereas its output variance is found to be 0.9 [Pa²]. Moreover, the total indices of the total resistance and compliance are almost zero. Therefore, we decided to firstly fix these two parameters on a constant value within their uncertainty domain (here the mean value, see *Table 1*), and secondly to redo the uncertainty and sensitivity analysis with the reduced input space (i.e., varying only Stroke Volume and Heart Rate). The results of this second analysis are shown in *Figure 5*. Both the expected value and the output variance are almost like the values found earlier, i.e., 2.3 Pa and 0.85 Pa² respectively. In essence, the re-definition of the input space did not result in different results when fixing the irrelevant parameters, hereby demonstrating the power of the sensitivity analysis. A reduced input space requires for example less samples to quantify the uncertainty and/or sensitivity analysis. Moreover, it can be observed that the relative contributions of the relevant parameters are hardly changed due to the re-defined of the input space (i.e., fixing irrelevant parameters).

⁷ Jose et al., 1970, DOI: 10.1093/cvr/4.2.160

⁸ Van Ooijen et al., 2012, DOI: 10.1148/rg.322115058

⁹ Wehrum et al., 2016, DOI: 10.1186/s12968-016-0252-3

¹⁰ Guigui et al., 2020, DOI: 10.21037/jtd.2020.02.20

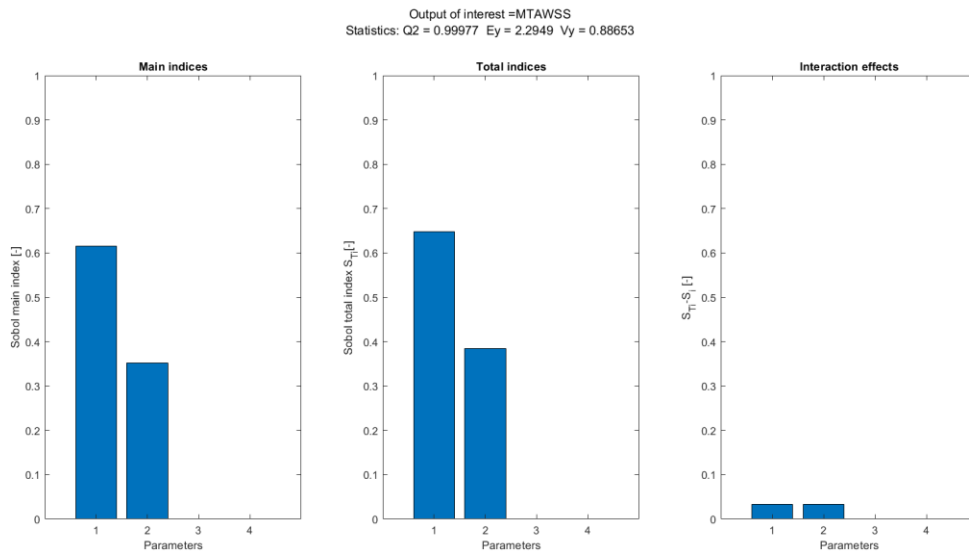


Figure 4: The sensitivity indices, the expected value, and the output variance for the first sensitivity analysis with the mean time averaged WSS as output of interest.

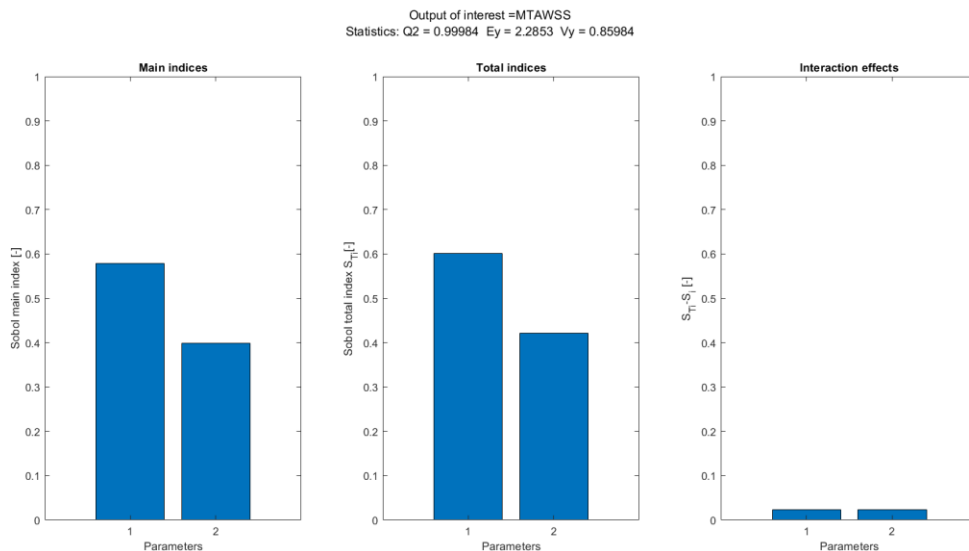


Figure 5: The sensitivity indices, the expected value, and the output variance for the second sensitivity analysis (and thus a re-defined input space) with the mean time averaged WSS as output of interest.

In contrary, the expected value and variance of the maximum arterial pressure (31 mmHg and 97 [mmHg²]) are different when performing the uncertainty and sensitivity analysis using the reduced input space (see Figure 6, Figure 7), where the expected value is 29 mmHg and the variance 66 [mmHg²]. This can be explained by the fact that the total compliance did not have a low total sensitivity index for this output of interest. In fact, this parameter could not be fixed to a constant within its uncertainty domain. Doing can decrease the accuracy of the expected value (unless it is luckily fixed on the exact value). The dimensionality, and the parameters that should span the input space, thus largely depend on the output of interest.

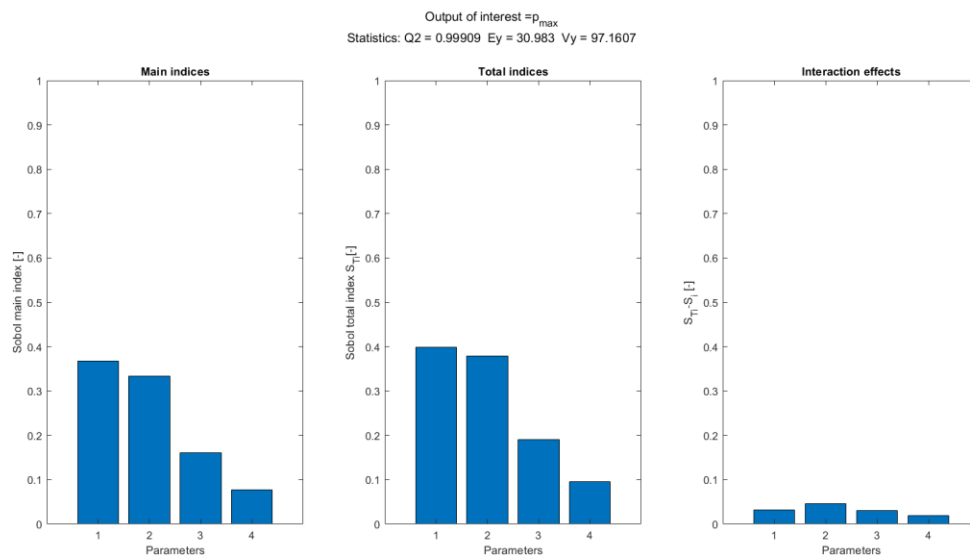


Figure 6: The sensitivity indices, the expected value, and the output variance for the first sensitivity analysis with the maximum pressure as output of interest.

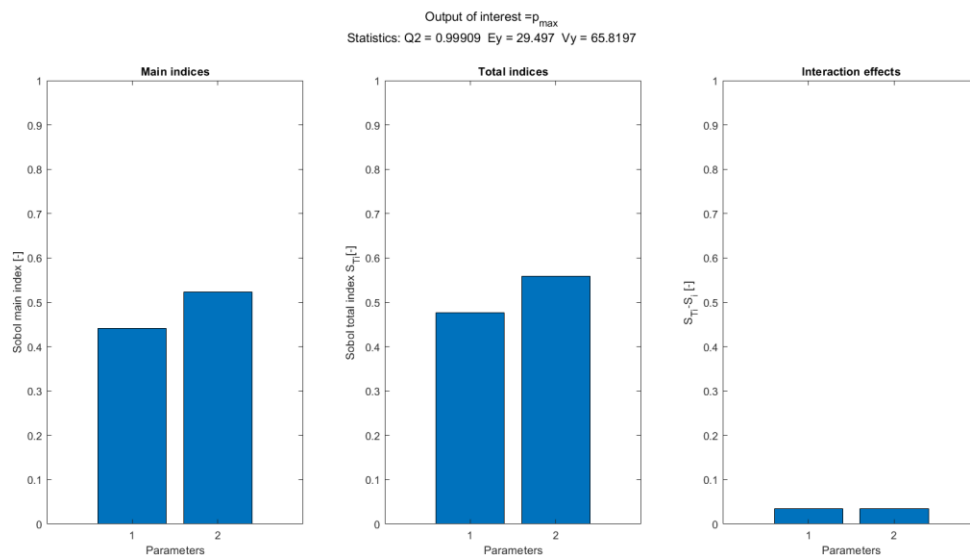


Figure 7: The sensitivity indices, the expected value, and the output variance for the second sensitivity analysis (and thus the re-defined input space) with the maximum pressure as output of interest.

Re-definition of input uncertainty domains

In this section the sensitivity analysis will be used to identify model parameters that are most rewarding to measure more accurately. In this case we will use the main sensitivity index. The parameter that has the largest value for the main index is the parameter that most likely results in the largest reduction in output uncertainty (variance). Moreover, this parameter will have the largest effect on the expected value estimations, especially in case of nonlinear, nonmonotone and nonadditive (interactions) relations between inputs and output.

Study setup

The analysis is here conducted on a hemodynamic model of the pulmonary artery with a pressure sensor implanted (see Figure 8). For calculation of the patient-specific haemodynamics within the pulmonary artery, a commercial finite volume solver (STAR-CCM+, Siemens PLM) is used. The patient-

specific geometry of the pulmonary artery, including the main, left and right pulmonary artery as well as smaller branching vessels is used as domain of interest. Within the domain of interest, the sensor is implanted via Boolean subtraction from the overall blood pool. As inlet boundary condition, the transient volume flow rate, which is generated from information on the patient-specific stroke volume and heart rate is used. At the outlets, a flow split of the volume flow going to the left and right pulmonary artery is specified. Blood is modelled as non-Newtonian fluid using a Carreau-Yasuda model. For this experiment, the threshold viscosity is varied to assess whether patient-specific modelling of the viscosity is required. Regularly, a viscosity of 0.0035 [Pa s] is used. As output parameters, the endothelial surface area of the pulmonary artery affected by low wall shear stresses ($< 0.5 \text{ Pa}$) due to the sensor and the hemodynamic forces (in axial direction) affecting the sensor during peak-systole are evaluated. For calculation of the hemodynamic forces, the surface integrals of the wall shear stresses at the sensor surface as well as the static pressure are calculated.

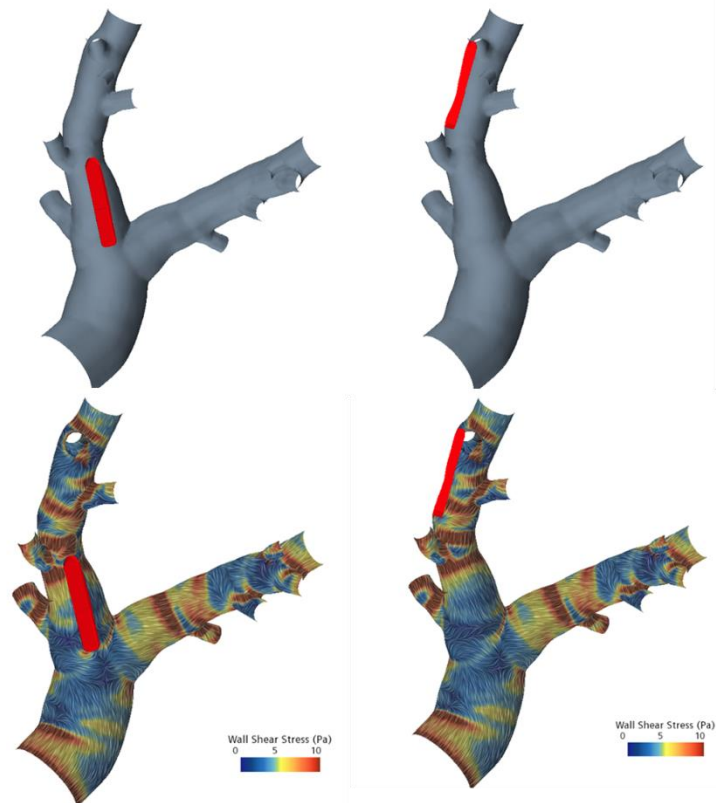


Figure 8: The setup of the model used for the uncertainty and sensitivity analysis. Top: The geometry and the pressure sensor inserted, bottom: exemplary results of wall shear stresses present.

The input parameters that are varied during the uncertainty and sensitivity analysis are the Heart Rate, Stroke Volume, Flow split (% of inflow to LPA), and dynamic blood viscosity. The ranges of the inputs are given in *Table 2*.

Input parameter	Ranges SA1	Ranges SA2
#1: Heart rate [bpm]	48 – 84	48 – 84
#2: Stroke Volume [ml]	27-135	54-108
#3: Flow split [% going to LPA]	40-60	40-60
#4: Dynamic Viscosity [mPa s]	3-4	3-4

Table 2: Input ranges for the uncertainty and sensitivity analysis (parameter prioritisation).

In this study, we reduce the uncertainty domain of the parameter with the highest main index and conduct a second uncertainty and sensitivity analysis. The reduction in uncertainty domain is for now arbitrarily chosen but can be used to show that our sensitivity analysis can select relevant parameters

to measure more accurately, leading to a reduction in output uncertainty. In addition, the effect of this reduced uncertainty domain on the expected value is evaluated.

Results and discussion

The first uncertainty analysis found an expected value for the area of low wall stress of approximately 3.0 [mm²] and an output variance of 15 [mm⁴]. The sensitivity indices are shown in *Figure 9*. The largest main index (~ 0.8) is found for the Stroke Volume. The input domain of this parameter is subsequently reduced for the second uncertainty and sensitivity analysis (see *Table 2* for the ranges used for this second analysis).

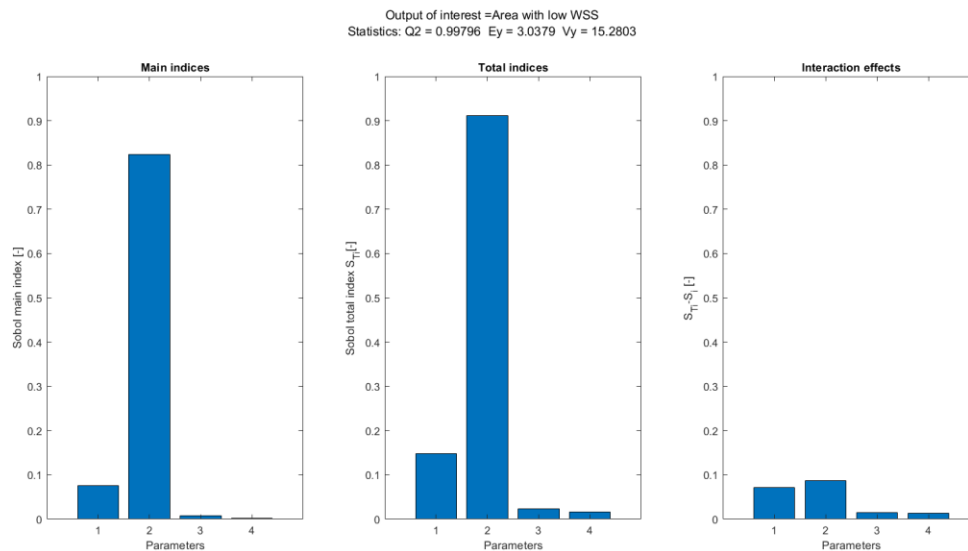


Figure 9: The sensitivity indices, the expected value, and the output variance for the first sensitivity analysis with the area of low WSS as output of interest.

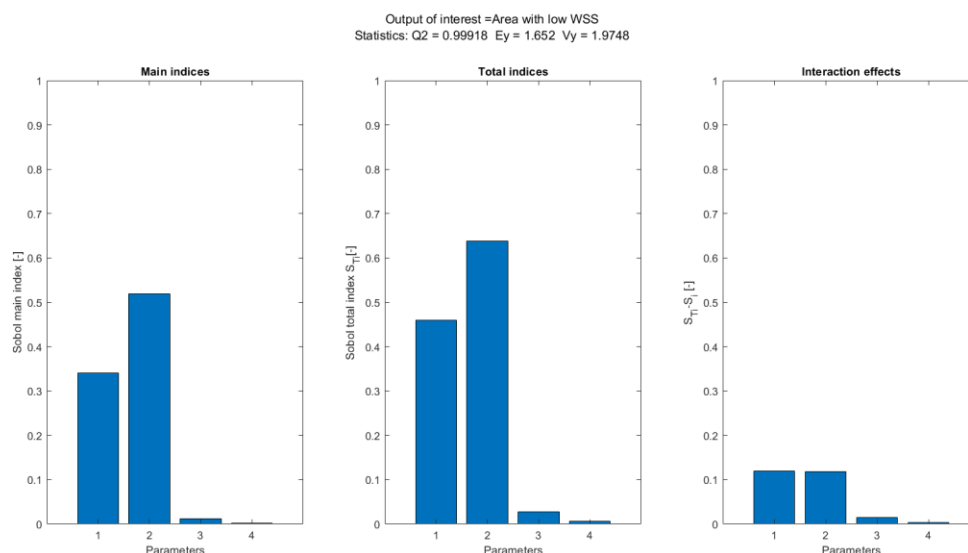


Figure 10: The sensitivity indices, the expected value, and the output variance for the second sensitivity analysis (and thus the re-defined input space) with the area of low WSS as output of interest.

In *Figure 10* we can observe by considering the sensitivity indices that the contribution of the heart rate to the total output uncertainty is significantly higher compared to the first exploration. This might

be understandable as the stroke volume is now more accurately determined and relatively gets a lower share of the total output uncertainty. In addition, you can see in *Figure 10* that the total output uncertainty ($\sim 2.0 \text{ mm}^4$) is indeed decreased. In addition, the expected value is significantly changed after re-definition of the input space.

Boxplots of the simulation data of both sensitivity analyses are given in *Figure 11*. Here it can be seen that the distribution in the first set of simulations is largely skewed, whereas the distribution of the second set of simulations is more symmetric. The model simulations of the first set in the outer tails of the distribution might be outliers and unrealistic but this needs to be assessed in future.

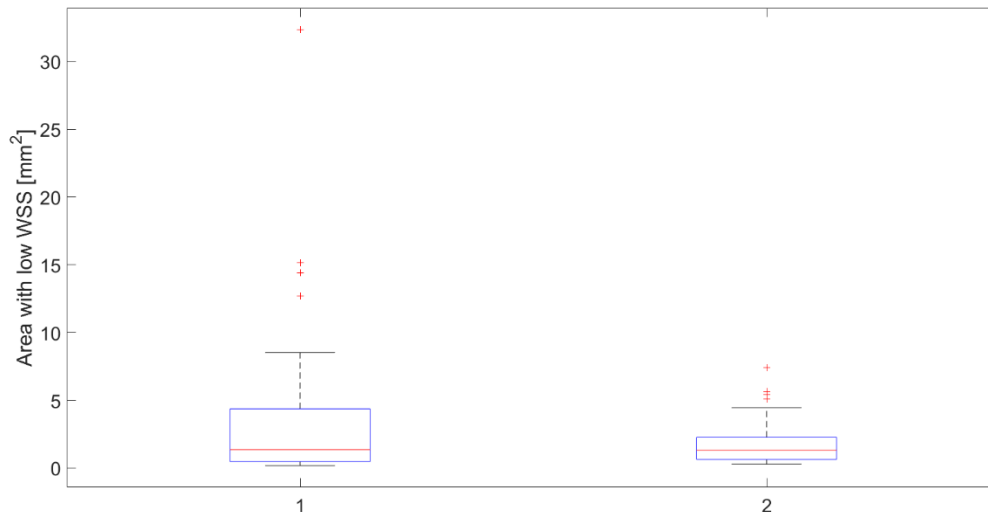


Figure 11: Boxplots showing the simulation data that was input for the agPCE. Note the outliers in especially the data set of the first uncertainty and sensitivity analysis (left).

In addition, we have performed uncertainty and sensitivity analysis for both the initial and re-defined input space while considering another output of interest, i.e., the pressure forces applied to the sensor. The results of the analysis with the initial input space are given in *Figure 12*. It can be observed that Stroke Volume has again the highest main index (almost 0.8). Therefore, we did the second analysis with the re-defined input space given in *Table 2*. The results of the second analysis are given in *Figure 13*. Now it can be observed that the expected values of both analyses are 4.5 [N], whereas the variance is 3.9 [N²] in the first analysis (initial input space) and more than halved (1.5 [N²]) in the second analysis.

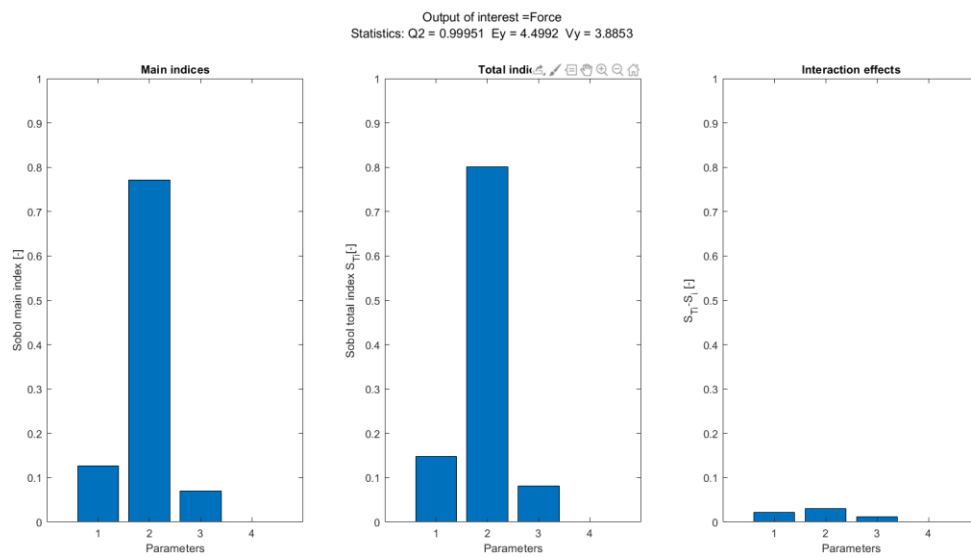


Figure 12: The sensitivity indices, the expected value and the output variance for the first sensitivity with the force applied to the sensor as output of interest.

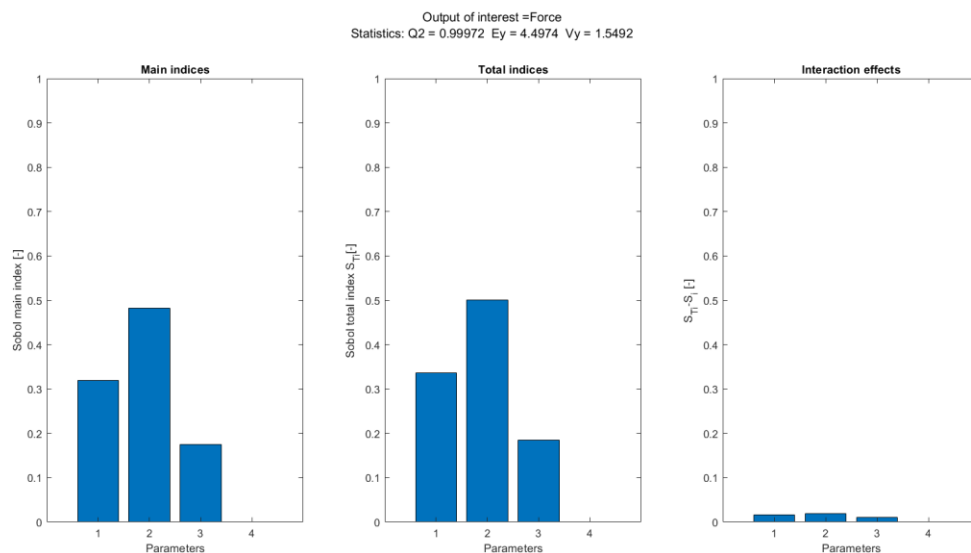


Figure 13: The sensitivity indices, the expected value, and the output variance for the second sensitivity (and thus the re-defined input space) with the force applied to the sensor as output of interest.

From the above discussion the relevance of uncertainty and sensitivity analysis for accurate estimations of model outputs and their variances becomes evident.

Re-definition of input space for virtual cohort generation

The re-definitions of the input space in the previous two sections are especially relevant during model personalization and patient-level validation. The re-definition of the input space in this section focusses on the re-definition of the input space for virtual cohort generation.

Study setup

Our approach to re-define the input space for virtual cohort generation is schematically depicted in Figure 14 and consists of the following steps: 1) sampling of the N-dimensional (sparse) input space; 2) evaluate the physiological models for each sample; 3) filter out model output realisations that are

non-physiological or outside a predefined region of interest; 4) define the distribution of the accepted (i.e., the re-defined input space) and non-accepted input samples. Note that the filter will be built based on a priori physiological knowledge and/or important parameters identified by regionalized sensitivity analysis (see D7.4). In this deliverable we have considered an aortic valve stenosis pressure drop larger than 300 mmHg as filter criterion for unrealistic outputs.

We have run our physiological model (surrogate model) for 3200 input samples that are obtained using Latin HyperCube sampling. All unrealistic model outputs are removed and thereafter the distribution of the input samples is investigated by means of a parallel orthogonal plot. This is a first preliminary exploration of a high dimensional input distribution obtained after filtering. The method considers “marginal distributions” and more advanced methods will be evaluated in the future.

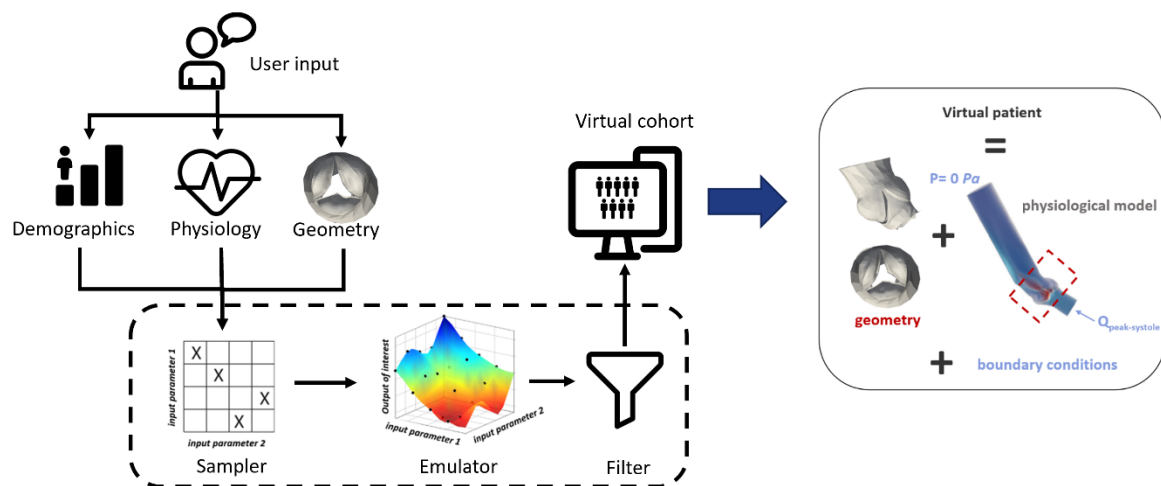


Figure 14: A schematic picture of the virtual cohort generator (left) and a typical example of a virtual patient, i.e., a geometry, a physiological model and proper parameters/boundary conditions (right).

Results and discussion

In total about 25% of all model evaluations resulted in unrealistic outputs. In Figure 15 a parallel orthogonal plot is shown for all simulations. The parallel axes of the plot represent either the ranges of the model output (pressure drop, completely at the right) or the input parameters (the α 's, scaling factor and the peak systolic flow, from left to right). For each single model realization lines are drawn that connect the specific output with the corresponding input values. The lines that are presented in Figure 15 represent the 10th, 50th and 90th percentile interval of all model realisations and inputs. In red this is depicted for the unrealistic inputs and outputs, whereas blue is used for the realistic ones. It can be observed that the inputs of both the realistic and unrealistic model realisations cover almost the full ranges for all input parameters except for parameter α_1 . For this parameter the percentile intervals of the two sets can be visually distinguished. The difference is even more pronounced when considering the 25th-75th percentile intervals of all simulations (Figure 16).

Based on these observations we have re-defined the input space by constraining the input range of α_1 to either the 10th-90th percentile or 25th-75th percentile interval. It is expected that sampling in these constrained regions will result in a lower number of unrealistic simulations. In fact, this is where we aim for, because our virtual cohort ultimately consists of an accurate input distribution that can be sampled to get realistic parameterizations and boundary conditions for our physiological model, which together form the virtual patients. Indeed, in Figure 17 we observe that the number of unrealistic model realisations reduce to an amount <0.5% when constraining the range of α_1 to the 25th and 75th percentile interval.

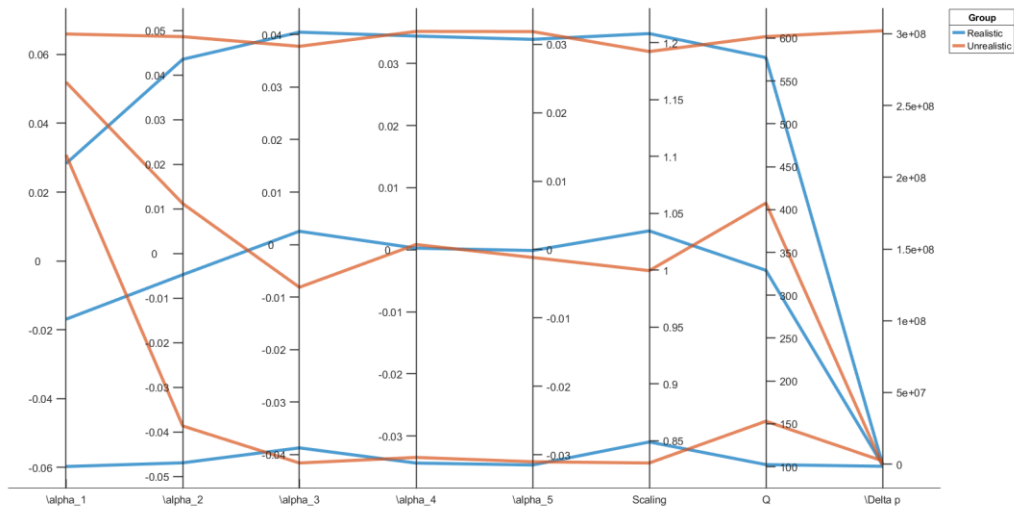


Figure 15: A parallel orthogonal plot showing the 10th to 90th percentile intervals for all components of the input samples and the corresponding model output realisations. These intervals are given for both realistic and unrealistic model outputs. Note that the value of the pressure drops in the plot seems to be large, but this is because the unrealistic outputs are also given, which can be much higher than the physiological (realistic pressure drops).

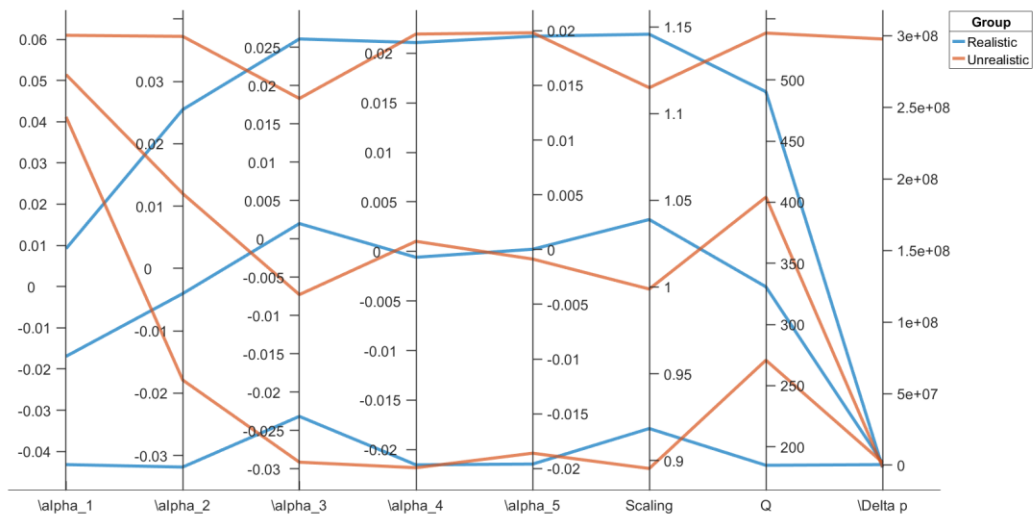


Figure 16: A parallel orthogonal plot showing the 25th to 75th percentile intervals for all components of the input samples and the corresponding model output realisations. These intervals are given for both realistic and unrealistic model outputs. The setup of the model used for the uncertainty and sensitivity analysis. Top: The geometry and the pressure sensor inserted, bottom: exemplary results of wall shear stresses present.

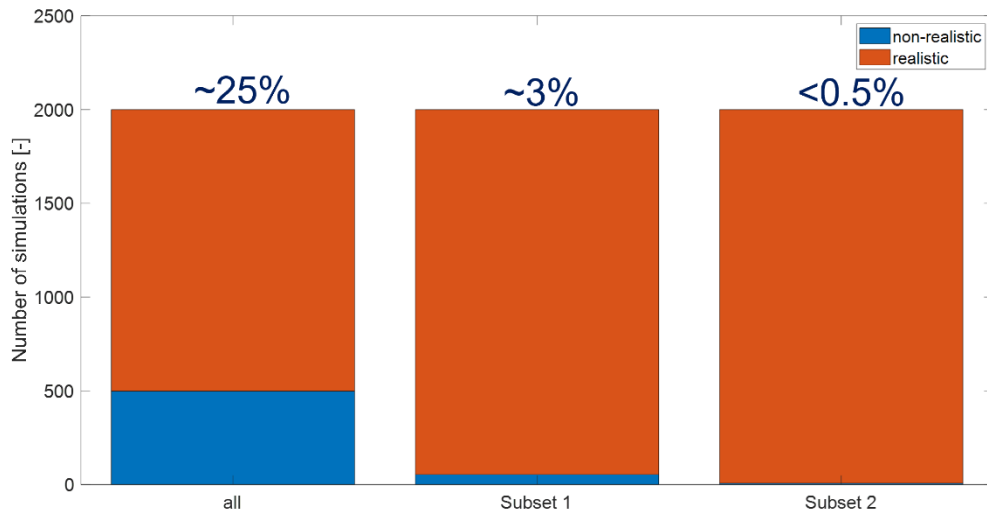


Figure 17: The number of unrealistic model realisations. On the left the situation without re-definition of the input space, whereas the middle and right illustrate the fraction of unrealistic simulations after re-defining the input space based on the 10th-90th percentile and 25th-75th percentile interval of parameter α_1 .

Next steps towards virtual cohort generation

In previous deliverables we have presented the methodology envisioned, the feasibility of the approach, and the availability and applicability of uncertainty and sensitivity analysis techniques. In the next phase of the project, we will now start with the development and validation of virtual cohorts. First, we will select the physiological model that is best suitable for our application and is available/has been developed in WP8 and WP9. Second, surrogate models are created for fast evaluations of the model which is needed for our filtering step. For the latter, our sensitivity analysis techniques will be used, complemented with physiological knowledge, to design the optimal acceptance/filtering criteria. Third, the different validation steps for virtual cohort validation will be done and ultimately the utility of the generated cohorts for device evaluation will be examined.